Integration of Nanostructured Multifunctional Surfaces into Analytical Chip

Andrej Oriňák, Renáta Oriňáková
University of P.J.Šafárik in Košice
Faculty of Sciences, Chemistry Institute, Department of Physical Chemistry
Moyzesova 11, 04154 Košice, Slovakia
andrej.orinak@upjs.sk, renata.orinakova@upjs.sk

Lenka Škantárová, Zuzana Nováková
Comenius University in Bratislava
Faculty of Science, Department of Analytical/Physical Chemistry
Mlynská Dolina CHII, Bratislava, Slovakia
lenka.skantarova@fns.uniba.sk

Jozef Radoňák
University of P.J.Šafárik in Košice
Faculty of Medicine, Trieda SNP 1
040 01 Košice, Slovakia
jozef.radonak@upjs.sk

***Abstract*—The nanostructures have currently received the great attractions for highly efficient and simultaneous analysis of a number of analytes. Outstanding optical property of noble metal nanostructures is a powerful phenomenon applied in chemical sensing. In this article, we introduce coupling of gold-capped silicone nanostructure prepared in fluidic channel with micro column high performance liquid chromatography. Micro column separation of the analytes was followed with an on-line deposition of effluent directly into a micro fluidic channel containing the deposited nanostructure. Effluent from micro column formed at gold-capped nanostructure a deposition trace, later analysed by surface-enhanced Raman spectro - scopy. The optical absorbance properties of nanostructure, the analytes in channel behavior as well optimization of chromatographic separation were investigated in this experiment. The surface enhancement factor 9.71 was obtained for rhodamine 6G in 30 μm wide fluidic channel. Optimum mobile phase composition was methanol/ water, 80/20, v/v. Detection of the analytes in 25 μm fluidic channel was affected with capillary forces during deposition process.**

Keywords-nanostructure; signal enhancement; SERS; integration; chip

I. INTRODUCTION

Micro fluidic systems are ideally suited for high-through -put chemical analysis since they offer high intensive analytical signal, consume minimum quantities of reagents, exhibit superior sensitivity and functionality compared to traditional micro-array techniques and can be integrated within complex work flows [1]. Detection of picomolar quantities of untagged oligonucleotides and polymerase chain reaction (PCR)-amplified desoxyribonucleic acid (DNA) samples with interferometric and localized surface plasmon resonance properties on gold nanostructure was demonstrated [2, 3]. An integrated analytical device composed of a microfluidic element and sensitive Raman spectrometer has been used with nanocolloid-based micro fluidic or metal nanostructure-embedded systems [4]. New methodology for enzyme assay using a sensitive and selective nanoparticle (AuNP)-enhanced time-of-flight secondary ion mass spectrometry (TOF SIMS) technique on self-assembled monolayers (SAMs) was reported [5]. Implementation of different functional nanostructures into fluidics was also documented [6-9]. The patterned micropads made of copper nanowires on silicon substrate showed the potential for application as chip to substrate interconnects [10]. Because metal deposited nanostructures usually do not provide any separation function this is in many cases substituted by chromatography or electrophoretic separation [11-12]. However, there are a lot of results documenting the analytes separation directly at a nanostructured surface [13-15]. The integration of fluidics and optics, as in flow-through nanohole arrays, has enabled increased transport of the analytes to sensing surfaces [16]. Uni-directional liquid spreading on asymmetric nanostructured surface [17] have enhanced surface wettability and enabled control of the liquid film thickness and final wetted shape. Liquid phase propagates in a single preferred direction and pins in all others. This is a key piece of chain coupled functional nanostructures in chip. As an example of multifunctional nanostructured surface can act silver nanorods array surface for on-a-chip separation and detection of chemical mixture by combining ultra – thin layer chromatography (UTLC) and surface-enhanced Raman spectroscopy (SERS). Limit of detection are between 10^{-5} – 10^{-6} M [18]. Another integration of the onedimensional nanostructures with the microsystems features with carbon nanotubes and nanowires [19].

In this article, we present the original results with functional gold – capped nanostructure that poses as a SERS nanodetector for the analytes former separated by micro column high performance liquid chromatogryphy (μHPLC). The separated analytes were deposited directly onto linearly moving micro fluidic channel with gold-capped nanostructure deposited inside. The separation conditions, a liquid phase behavior after micro fluidic channel dropping as

 ISBN: 978-1-61208-214-1

well SERS sensitivity were studied for future implementation in analytical microsystems or chips (with integrated multifunctional nanostructures; separation, unidirectional phase propagation, detection, etc.).

II. MATERIALS AND METHODS

A. Chemicals

All the chemicals used (acetonitrile, dioxane, methanol, rhodamine 6G (R6G) and rhodamine B (RB)) were purchased from Alfa Aesar GmbH (Germany). All of them were of an analytical grade of purity. The μHPLC mobile phases were mixed in the proportions: methanol: water / 80:20 (v/v); acetonitrile: water / 80:20 (v/v); dioxane: water/ 80:20 (v/v) and also filtered through 0.2μm filters to prevent obturation of a microcolumn. The structural formulas of both rhodamines are given at Figures 1 and 2.

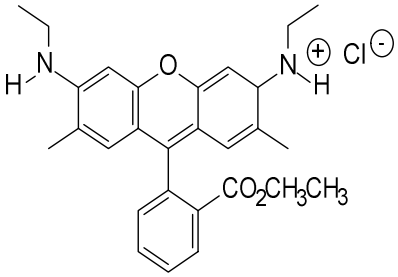

Figure 1. Structural formula of R6G, M.w. 479.01g/mol.

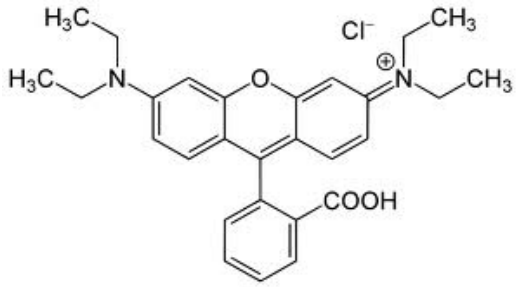

Figure 2. Structural formula of RB, M.w. = 479.21 g/mol.

B. Materials and methods

The black silicon nanostructure was prepared by advanced silicon etching (ASE) (STS MESC Multiplex), etching the plain silicon wafer with tiohexafluoride /oxygen plasma. The parameters of the etching gases and the conditions of plasma: SF_6 flow – 99 standard cubic centimeter per minute (sccm), O_2 flow – 90 sccm, coil power – 2800 W, platen power – 16 W, pressure process – 5.06Pa, pressure base – 12.53Pa, time – 4 minutes. After the etching process, the substrate was covered with the layer of noble metal (Au) by e-beam deposition process. Single side polished silicon wafers with diameter 100 mm and thickness 525 μm ± 25 μm [14].The different channels with integrated gold - capped nanostructures are given at Figure 3.

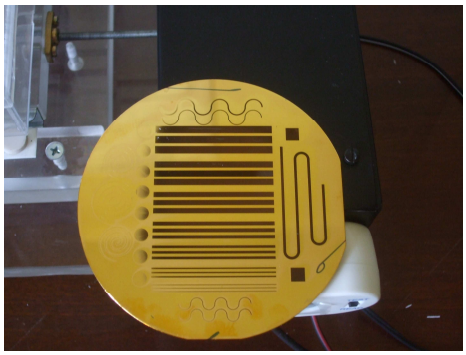

Figure 3. The microfluidic channels (different width) with implemented silicone gold - capped nanostructure inside.

In this experiment were used the micro channels 25 μm deep and 25 or 30 μm wide. Micro column high- performance liquid chromatography (μHPLC) was performed by Shimadzu high performance liquid micro pump LC-5A (Shimadzu Corporation, Kyoto Japan). LC-5A is a delivering system of mobile phase for μHPLC using a small plunger reciprocating pump. In this instrument, employment of the constant displacement with quick return (CDQR) enables pulsation-free and stable flow even with a single plunger. CDQR means delivery solvent at a constant rate and with high speed suction. This instrument has a wide range of flow rate setting from 1 μl/min. to 9.900 μl/min. Specific is a high delivery pressure of 500 kg/cm^2 maximum. For a liquid chromatography system, a micro volume high pressure injector model 7520 (Rheodyne) with 0.5μL sample loop has been used. Separation of both the rhodamines was done at a micro column Prote–Col C_{18} (SGE Analytical, Australia), 150 mm long, 300 μm column internal diameter and pore size of 12 nm. Home made column holder and deposition device cell let move channel with constant rate and let effluent from micro column to be deposited into a fluidic channel. Complete instrumental set up is given at Figure 4.

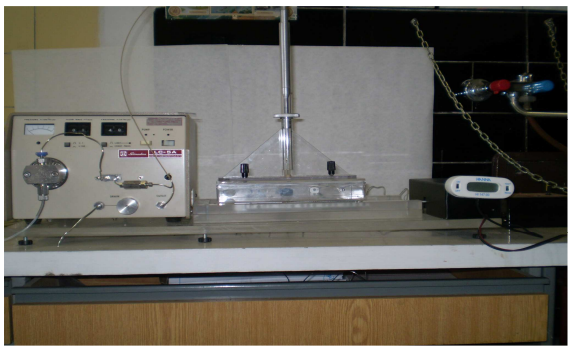

Figure 4. Analytical miniaturised system with micropump(left), separation microcolumn (middle) and fluidic channel with nanostructure in deposition cell (middle bottom).

 ISBN: 978-1-61208-214-1

Capillary μHPLC column was tested in the following conditions: mobile phase: acetonitrile/ water 60:40, v/v; mobile phase flow rate: 4 μL/ min; sample injection volume: 0.02 μL. A concentration of both the analytes in the mixture was 1 mmol/L. The Raman spectra were obtained using an i-Raman® instrument (B&W Tek). Excitation was provided by a 532.1 nm Nd:YAG laser. The laser power at the sample was approximately 9 mW. The acquisition time for each accumulation was 5 s.

III. RESULTS AND DISCUSSION

A. μHPLC mobile phase optimization

The optimization of μHPLC mobile phase composition has been based on the preliminary results obtained from thin layer chromatography (TLC) as documented in table 1. The retardation factor R_f, was calculated for a each spot according to the following formula:

$$R_f = a/b \quad (1)$$

where *a, b* are the distance moved by the sample component (a) and the solvent mixture (b). The best separation efficiency has been obtained by applying mobile phase methanol (MeOH) - water (80/20, v/v). The worse separation efficiency was obtained with dioxane- water mobile phase. The analytes were spread when acetonitrile-water mobile phase applied. Separation was controlled visually by a deposition of μHPLC effluent directly to white adsorption substrate sheet (Figure 5). The first eluted was RB, that is pink- violet coloured, and as a second one R6G characteristic with orange-red coloured spot (Figure 5).

TABLE I. THE RESULTS OF SEPARATION OF RHODAMINES MIXTURE (DEPOSITION LINEAR VELOCITY WAS 2.7 MM/MIN.).

Mobile phase	***Cell Temperature [°C]***	***Pump Pressure [x 100 kg/cm²]***	**Rhodamine R_F**	
			R6G	*RB*
MeOH-water 80:20	26.3	1.9	0.23	0.30
ACN - water 80:20	25.3	0.7	0.35	0.16
Dioxane: water 80:20	27.6	1.8	0.29	0.51

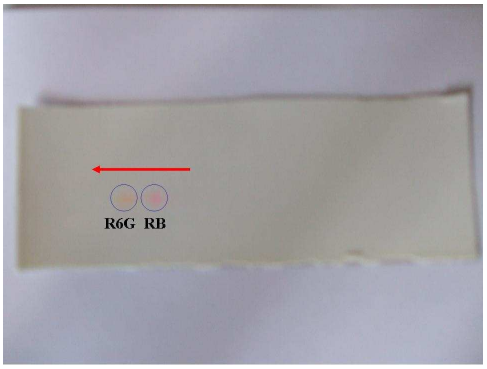

Figure 5. White substrate sheet with deposited effluent of micro column separated R6G and RB with MeOH-water mobile phase (80:20, v/v). Red arrow signals a micro column effluent deposition direction.

In the next experiment, the same mixture of rhodamines has been separated with the optimized mobile phase. The analytes eluted were continuously deposited into linearly moving microfluidic channel, containing functional gold-capped nanostructure that can enhance analytical signal in SERS. A micrograph of a cut microfluidic channel with a deposited nanostructure surface is given in Figure 6. Optimum effluent deposition rate as well a mobile phase flow rate were established at 2.7 mm/min. and 6 μL /min., simultaneously.

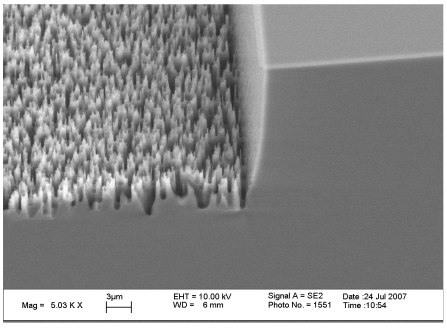

Figure 6. Micrograpg of silicon etched gold – capped nanostructure in fluidic channel.

B. SERS detection of the R6G and RB at a gold- capped nanostructure

Raman spectra of R6G and RB stock solutions at a gold – capped nanostructured surface are given at the Figures 7 and 8, respectively. There are the small differences in Raman shift positions. Significant is a lower intensity of the RB Raman bands to compare with R6G one. The Raman shift intensities were used for calculation of Raman signal enhancement for both the rhodamines at nanostructure in fluidic microchannel. The enhancement factor, *fe*, was calculated according to the following formula:

$$f_e = \frac{c_{ref}}{c_{sample}} \cdot \frac{I_{sample}}{I_{ref}} \quad (2)$$

 ISBN: 978-1-61208-214-1

where c_{ref} and c_{sample} are the reference concentration and sample concentrations, respectively, and I_{ref} is the signal intensity of the respective Raman peak.

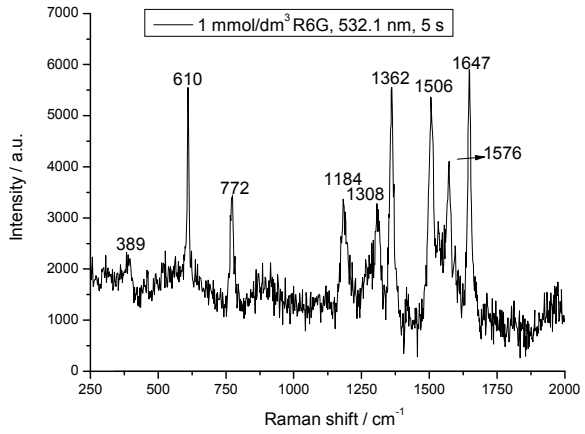

Figure 7. Raman spectrum of R6G at the gold-capped nanostructure.

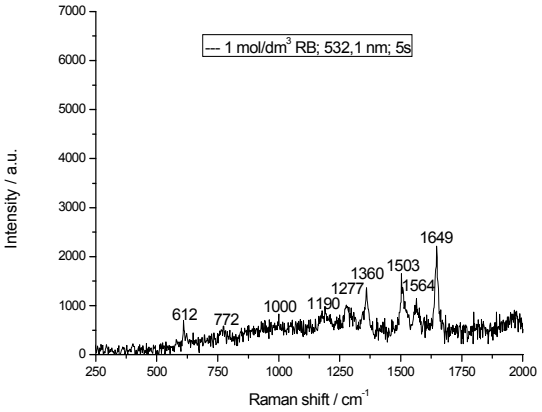

Figure 8. Raman signal intensity of RB stock solution at gold-capped nanostructure.

C. *SERS detection of the R6G and RB at a gold- capped nanostructure after a separation at micro column and deposition of an effluent into the fluidic microchannels*

Fluidic channels with the implemented gold-capped nanostructure were 25 or 30 μm wide and Raman signal shift was monitored for more intensive shift bands: 610, 1362, 1649 and 1506 cm^{-1} for R6G. Simultaneously, for RB the following Raman shift bands were concerned for data evaluation: 772, 1190, 1277 and 1564 cm^{-1}. From Figure 9, resulted position of R6G in the 30μm wide channel confirmed by SERS spectrum. Signal enhancement factor f_e for R6G was determined at value 9.71 (1362 cm^{-1}) and 7.29 (1564 cm^{-1}). It is less than reported in the experiments at surface nanosatructure [20].

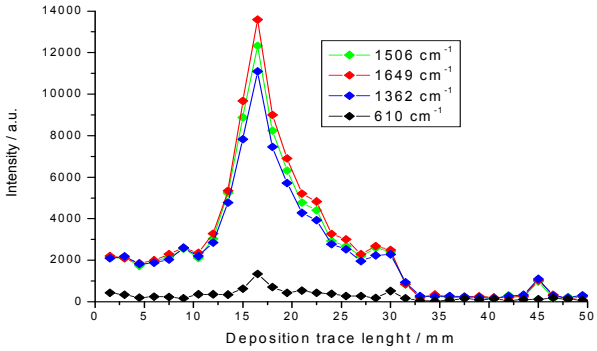

Figure 9. Signal intensity of Rama shift bands of separated and deposited rhodamine 6G at fluidic channel with gold-capped nanostructure. Mobile phase : MeOH:water , 80:20, v/v; 30μm channel width.

In a Figure 10, it is demonstrated detection of RB after chromatographic mixture separation and deposition of an effluent into a fluidic microchannel. The values of a signal enhancement f_e, were lower, ranging from 2.45 (1277 cm^{-1}) to 2.30 (1564 cm^{-1}). This is corresponding to difference in the Raman shift intensities (Figure 7, 8). In 20 μm wide channel was measured a lower Raman signal enhancement. It was in the range from 0.67 (1362 cm^{-1}) to 0.59 (1564 cm^{-1}) for R6G while only 0.19 (1277 cm^{-1}) and 0.18 (1564 cm^{-1}) in case of RB, which means no enhancement at all. An effluent deposition in this channel was probably strongly effected with a dispersion of the analytes separated from column directly at nanostructure. A mass of separated analyte was deposited in the length deposition trace. From the next results, it was confirmed that both the rhodamine analytes can be detected at nanostructure directly into a fluidic channel. Moreover, functional nanostructure affected signal enhancement for both the analytes. A position of RB was spread and no so sharp as given at Figure 9 for R6G.

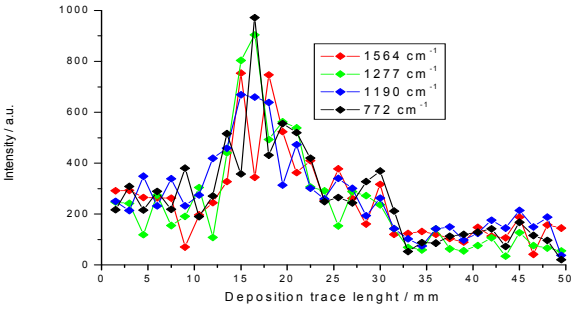

Figure 10. Rama signal shift of a separated and deposited RB in fluidics channel with gold-capped nanostructure. Mobile phase MeOH : water , 80:20, v/v; 30μm channel width.

 ISBN: 978-1-61208-214-1

There were also observed the special driven processes coupled with capillary force in microchannel and an analyte mass transfer that will be studied later on. The limits of detection, however, are fundamentally limited by local analyte concentration.

IV. CONCLUSIONS

A gold - capped silicon etched nanostructure has been deposited directly into microfluidic channel. With special μHPLC system and deposition device the separated rhodamines 6G and B have been deposited directly into integrated nanostructure in fluidic channel after chromatographic separation. From Raman spectroscopy band shift results it was found that rhodamine 6G can be good detected at gold–capped nanostructure in a micro-channel due to analytical signal enhancement, forced by nanostructure. Thinner, 20 μm wide microfluidic channel did not enable the equivalent signal enhancement. Generally, a Raman signal enhancement value was lower as in the measurements obtained out of microfluidic channel at the same defined nanostructure. Integration of functional nanostructure into a microfluidic channel enabled separated analytes deposition, spectroscopic detection, position scan, comparison of signal enhancement as well study of behaviou in this environment. The integrated nanostructures generate new functions that were directly included in an analytical miniaturized systems to form an analytical base for a chip or sensor integration.

ACKNOWLEDGMENT

The authors wish to thank MŠ SR VEGA 1/0211/12, APVV-0280-11 for financial support and Dr. I.Talian for silicon gold-capped nanostructure preparation.

REFERENCES

[1] S. Cho, D.-K. Kang, J. Choo, A. J. deMello, and S.-I. Chang, “Recent advances in microfluidic technologies for biochemistry and molecular biology”, BMB Reports vol. 44 pp. 705-712, 2011.

[2] D.-K. Kim, K. Kerman, M. Saito, R. R. Sathuluri, T. Endo, S. Yamamura, Y.-S. Kwon,and E. Tamiya, “Label-free DNA biosensor based on localized surface plasmon resonance coupled with interferometry”, Anal.Chem., vol. 79, pp. 1855-1864, 2007.

[3] D.-K. Kim, K. Kerman, S. Yamamura, Y.-S. Kwon, Y. Takamura,and E. Tamiya,”Label-free optical detection of protein antibody-antigen interaction on an capped porous anodic alumina layer chip”, Japan. J.Appl. Phys., vol. 47, pp. 1351-1354, 2008..

[4] C. Lim, J. Hong, B. G. Chung, A. J. deMello, and J. Choo,”Optofluidic platforms based on surface-enhanced Raman scattering”,Analyst, vol. 135, pp. 837-844, 2012.

[5] Y.-P. Kim, E. Oh, H. K. Shon, D. W. Moon, T. G. Lee, and H.-S. Kim,” Gold nanoparticle-enhanced secondary ion mass spectrometry and its bio-applications”, Appl. Surf.Sci. vol. 255, pp. 1064-1067, 2008.

[6] T. O. Dare, H. A. Davies, J. A. Turton, L. Lomas, T. C. Williams, and M. J. York,”Application of surface-enhanced laser desorpti - on/ionization technology to the detection and identification of urinary parvalbumin-alpha: a biomarker of compound-induced skeletal muscle toxicity in the rat”, Electrophoresis, vol. 23, pp. 3241-3251, 2002.

[7] S.-W. Ryu, Ch.-H. Kim, J.-W. Han, Ch. Jung, H. G. Park,and Y. K. Choi,” Gold nanoparticle embedded silicon nanowire biosensor for applications of label-free DNA detection”, Biosen. Bioelect., vol 25 pp. 2182-2185, 2010.

[8] J. C. Aspas, B. Heeg, B. Bescós, V. Zapata, and A. G. Ureña,”Vibrational enhancement on beam-surface ionization processes”, Faraday Disc., vol. 96, pp. 227-233, 1993.

[9] H. Wang, X. Luo, H. Yao, C. Du, Z. Y. Zhao, and S. Zhu,”Key technologies for LSPR-sensing microfluidic biochip”, art. No. 67241V, Proceedings of the society of photo-optical instrumentation engineers, 2007.

[10] G. Sharma, C. S. Chong, L. Ebin, V. Kripesh, C. L. Gan, and C. H. Sow,” Patterned micropads made of copper nanowires on silicon substrate for application as chip to substrate interconnects”, Nanotech. vol. 18, pp. 105-107, 2007.

[11] L. Geng, P. Jiang, J. Xu, B. Che, and F. Qu, Y. Deng,”Applications of Nanotechnology in Capillary Electrophoresis and Microfluidic Chip Electrophoresis for Biomolecular Separations”,Progr. Chem.,vol. 21, pp.1905-1921, 2009.

[12] R. M. Connatser, L. A. Riddle, and M. J. Sepaniak,”Metal-polymer nanocomposites for integrated microfluidic separations and surface enhanced Raman spectroscopic detection” J. Sep. Sci., vol. 27, pp. 1545-1550, 2004.

[13] L. W. Bezuidenhout, and M. J. Brett,”Ultrathin layer chromatography on nanostructured thin films”, J.Chromatogr. A, vol. 1183, pp. 179-185, 2008.

[14] A. Fonverne, F. Ricoui, C. Demesmay, C. Delattre, A. Fournier, J. Dijon, and F. Vinet,”In situ synthesized carbon nanotubes as a new nanostructured stationary phase for microfabricated liquid chromatographic column”, Sens. Actu. B, vol. 129, pp. 510 – 517, 2008.

[15] M. S. Haque, K. B. K. Teo, N. L. Rupensinghe, S. Z. Ali, I. Haneef, S. Maeng, J. Park, F. Udrea, and W. I. Milne,”On-chip deposition of carbon nanotubes using CMOS microhotplates”, Nanotech. vol. 19, pp.458-462, 2008.

[16] C. Escobedo, A.G. Brolo, R. Gordon, and D. Sinton, ”Optofluidic Concentration: Plasmonic nanostructure as concentrator and sensor, Nano Lett. vol. 12, pp.1592-1596, 2012.

[17] K. H. Chu, R. Xiao, and E. N. Wang,”Uni-directional liquid spreading on asymmetric nanostructured surfaces”, Nat. Mat., vol 9, pp. 413-417, 2010.

[18] J.Chen, J.Abell, Y-W. Huang and Y.Zhao,“On.Chip ultra-thin layer chromatography and surface enhanced Raman spectroscopy“,Lab on a Chip, in press.

[19] B.E. Alaca,”Integration of one-diemnsional nanostructures with Microsystems: an overview”,Int.Mat.Rev. vol.54, pp.245-260, 2009.

[20] I. Talian, M. Aranyosiová, A. Oriňák, D. Velič, D. Haško, D. Kaniansky, R. Oriňáková, and J. Hübner,”Functionality of novel black silicon based nanostructured surfaces studied by TOF SIMS”, Appl. Surf. Sci., vol. 256, pp. 2147-2154, 2010.

 ISBN: 978-1-61208-214-1